Respiration, heartbeat, and conscious tactile perception

Abbreviated title: Respiration, heartbeat, and tactile perception

Martin Grund[1], Esra Al[1,2], Marc Pabst[1], Alice Dabbagh[1,3], Tilman Stephani[1,4], Till Nierhaus[1,5], and Arno Villringer[1,2]

[1]Department of Neurology, Max Planck Institute for Human Cognitive and Brain Sciences, 04103 Leipzig, Germany

[2]MindBrainBody Institute, Berlin School of Mind and Brain, Charité – Universitätsmedizin Berlin and Humboldt-Universität zu Berlin, 10099 Berlin, Germany

[3]Pain Perception Group, Max Planck Institute for Human Cognitive and Brain Sciences, 04103 Leipzig, Germany

[4]International Max Planck Research School NeuroCom, 04103 Leipzig, Germany

[5]Neurocomputation and Neuroimaging Unit, Department of Education and Psychology, Freie Universität Berlin, 14195 Berlin, Germany

Corresponding author: Martin Grund, Max Planck Institute for Human Cognitive and Brain Sciences, Stephanstr. 1A, 04103 Leipzig, Germany (mgrund@cbs.mpg.de)

Number of pages: 43

Number of figures: 7

Number of words for *Abstract*: 243; *Introduction*: 649; *Discussion*: 1375

Conflict of Interest: The authors declare no competing financial interest.

Acknowledgements: The research was funded by the Max Planck Society. We thank Sylvia Stash for her data acquisition support; Mina Jamshidi Idaji for data analysis advice; and Heike Schmidt-Duderstedt for preparing the figures for publication.

Abstract

Cardiac activity has been shown to interact with conscious tactile perception: Detecting near-threshold tactile stimuli is more likely during diastole than systole and heart slowing is more pronounced for detected compared to undetected stimuli. Here, we investigated how cardiac cycle effects on conscious tactile perception relate to respiration given the natural coupling of these two dominant body rhythms. Forty-one healthy participants had to report conscious perception of weak electrical pulses applied to the left index finger (yes/no) and confidence about their yes/no-decision (unconfident/confident) while electrocardiography (ECG), respiratory activity (chest circumference), and finger pulse oximetry were recorded. We confirmed the previous findings of higher tactile detection rate during diastole and unimodal distribution of hits in diastole, more specifically, we found this only when participants were confident about their detection decision. Lowest tactile detection rate occurred 250-300 ms after the R-peak corresponding to pulse-wave onsets in the finger. Inspiration was locked to tactile stimulation, and this was more consistent in hits than misses. Respiratory cycles accompanying misses were longer as compared to hits and correct rejections. Cardiac cycle effects on conscious tactile perception interact with decision confidence and coincide with pulse-wave arrival, which suggests the involvement of higher cognitive processing in this phenomenon possibly related to predictive coding. The more consistent phase-locking of inspiration with stimulus onsets for hits than misses is in line with previous reports of phase-locked inspiration

47 to cognitive task onsets which were interpreted as tuning the sensory system for
48 incoming information.

49

50 **Keywords:** respiration, cardiac cycle, interoception, tactile perception,
51 electrocardiogram, pulse oximetry

Significance statement

Mechanistic studies on perception and cognition tend to focus on the brain neglecting contributions of the body. Here, we investigated how respiration and heartbeat influence tactile perception: We show that inspiration locked to expected stimulus onsets optimizes detection task performance and that tactile detection varies across the heart cycle with a minimum 250-300 milliseconds after heart contraction, when the pulse reaches the finger. Lower detection was associated with reduced confidence ratings, indicating – together with our previous finding of unchanged early ERPs - that this effect is not a peripheral physiological artifact but a result of higher cognitive processes that model the internal state of our body, make predictions to guide behavior, and might also tune respiration to serve the task.

Introduction

Our body senses signals from the outer world (exteroception), but also visceral signals from inside the body (interoception) and it has been shown that these two continuous types of perception interact (Critchley and Harrison, 2013; Critchley and Garfinkel, 2015; Babo-Rebelo et al., 2016; Azzalini et al., 2019). For example, we have recently shown that tactile perception interacts with cardiac activity as conscious detection of near-threshold stimuli was more likely towards the end of the cardiac cycle (Motyka et al., 2019; Al et al., 2020) and was followed by a more pronounced deceleration of heart rate as compared to missed stimuli (Motyka et al., 2019). In line with increased detection during later cardiac phases (diastole), late (P300) cortical somatosensory evoked potentials (SEPs) were also higher during diastole as compared to systole (Al et al., 2020). A similar cardiac phase-dependency has also been revealed for visual sampling: microsaccades and saccades were more likely during systole, whereas fixations and blinks during diastole (Ohl et al., 2016; Galvez-Pol et al., 2020). Following an interoceptive predictive coding account, the very same brain model that predicts cardiac-associated bodily changes and suppresses their access to consciousness might suppress perception of external stimuli which coincide with those changes and modulate the generation of actions (Seth and Friston, 2016; Kunzendorf et al., 2019; Allen et al., 2019). Yet, which bodily changes are the main driver for the cardiac-related perceptual suppression effect remain to be determined.

Another dominant body rhythm that can even be regulated intentionally in contrast to cardiac activity is the respiration rhythm (Azzalini et al., 2019). Also for respiration, which naturally drives and is driven by cardiac activity (Kralemann et al.,

2013; Dick et al., 2014), phase-dependency of behavior and perception has been reported. For instance, self-initiated actions were more likely during expiration, whereas externally-triggered actions showed no correlation with the respiration phase (Park et al., 2020). Furthermore, inspiration onsets were reported to lock to task onsets which resulted in greater task-related brain activity and increased task performance for visuospatial perception, memory encoding and retrieval, and fearful face detection (Huijbers et al., 2014; Zelano et al., 2016; Perl et al., 2019). Locked inspiration was interpreted as tuning the sensory system for upcoming information (Perl et al., 2019). Thus, inspiration might also be beneficial for conscious perception and could be timed to paradigms instead of modelled as noise (heartbeat) within an interoceptive predictive coding framework. While cardiac activity and respiration are closely interdependent, it remains unclear how they jointly shape perceptual processes.

Our present study combined the observation of cardiac and respiratory activity with a paradigm that asked participants to report (a) conscious perception of weak electrical pulses applied to their left index finger and (b) their decision confidence. Decision confidence was assessed to identify the potential role of metacognition in cardiac cycle effects. As we have previously shown that greater tactile detection during diastole corresponded to increased perceptual sensitivity and not to a more liberal response criterion (Al et al., 2020), we expected the cardiac cycle effect not to be a side-effect of unconfident perceptual decisions. Recently, afferent fibers in the finger have been reported to be modulated by cardiac pressure changes which the

brain has to ignore or filter out (Macefield, 2003). Thus, we measured pulse oximetry to investigate whether peripheral physiological changes in the finger caused by the blood pulse wave coincided with lower tactile detection during systole. Furthermore, we tried to capture early SEPs at the upper arm to rule out differences in (peripheral) SEP amplitudes as explanation for altered conscious tactile perception across cardiac or respiratory cycles.

This study setup was intended to address the following research questions:

- Does the interaction of cardiac activity and conscious tactile perception depend on decision confidence?
- How is the relationship between decreased tactile detection and the kinetics of the pulse wave in the finger?
- Does conscious tactile perception vary across the respiratory cycle?

Methods

Participants

Forty-one healthy humans (21 women, mean age = 25.5, age range: 19-37) participated in the study. Participants were predominantly right-handed with a mean laterality index of 90, *SD* = 17 (Oldfield, 1971). For four participants, the mean laterality index was not available.

Ethics statement

All participants provided an informed consent. The experimental procedure and physiological measurements were approved by the ethics commission at the medical faculty of the University of Leipzig.

Experimental design and statistical analysis

The experiment was designed to capture tactile detection of near-threshold stimuli (50% detection) and trials without stimuli (0% detection) across the cardiac and respiratory cycle. This resulted in three main stimulus-response conditions: (a) correct rejections of trials without stimulation, (b) undetected (misses), and (c) detected near-threshold stimuli (hits). False alarms (yes-responses) during trials without stimulation were very rare (mean FAR = 6%, *SD* = 6%) and thus not further analyzed. Additionally, participants reported their decision confidence which allowed us to split trials by confidence.

We applied circular statistics to investigate whether conscious tactile perception was uniformly distributed across the cardiac and respiratory cycle or showed unimodal patterns. For each stimulus onset, the temporal distances to the

145 preceding R-peak and inspiration onset were calculated and put in relation to its
146 current cardiac and respiratory cycle duration measured in degrees. Following for
147 each participant, these angles were averaged for hits, misses, and correct rejections.
148 For each stimulus-response condition, the resulting distributions of mean angles were
149 tested across participants with the Rayleigh test for uniformity from the R package
150 "circular" (Version 0.4-93). The application of circular statistics had two advantages:
151 First, it accounted for cardiac and respiratory cycle duration variance within and
152 between participants. Second, it allowed us to determine phases when detection
153 differed without having to rely on arbitrary binning. However, it assumed that the
154 different phases of the cardiac and respiratory cycle behave proportionally the same
155 when cycle duration changes. That is why we complemented the circular statistics
156 with a binning analysis that investigated the near-threshold detection rate for fixed
157 time intervals relative to the preceding R-peak and inspiration onset.

158 In repeated-measures ANOVAs, Greenhouse-Geisser correction was used to
159 adjust for the lack of sphericity. Post-hoc *t*-tests p-values were corrected for multiple
160 comparisons with a false discovery rate (FDR) of 5% (Benjamini and Hochberg, 1995).

161

162 **Data and code availability**

163 The code to run and analyze the experiment is available at
164 http://github.com/grundm/respirationCA. The behavioral and physiological data
165 (electrocardiogram, respiration, and oximetry) can be shared by the corresponding
166 author upon request if data privacy can be guaranteed.

Stimuli and apparatus

Somatosensory stimulation was delivered via steel wire ring electrodes to the left index finger with a constant current stimulator (DS5; Digitimer, United Kingdom). The anode was placed on the middle phalanx and the cathode on the proximal phalanx. The stimuli were single square-wave pulses with a duration of 0.2 ms and an individually-assessed near-threshold intensity (mean intensity = 1.95 mA, range: 0.76-3.17 mA). The stimulator was controlled by the waveform generator NI USB-6343 (National Instruments, Austin, Texas) and custom MATLAB scripts using the Data Acquisition Toolbox (The MathWorks Inc., Natick, Massachusetts, USA).

Behavioral paradigm

Participants had to report whether they perceived an electrical pulse and whether this yes/no-decision was confident or not. The experiment was separated into four blocks. Each block consisted of 150 trials. Participants received a near-threshold stimulus in 100 trials (mean intensity = 1.96 mA, range: 0.76-3.22 mA). In 50 trials, there was no stimulation (33% catch trials). The order of near-threshold and catch trials was pseudo-randomized for each block and participant. In total, there were 400 near-threshold and 200 catch trials.

Each trial started with a black fixation cross (black "+") for a counterbalanced duration of 1.0-2.0 s (Figure 1). It was followed by a salmon-colored fixation cross (0.62 s) to cue the stimulation at 0.5 s after the cue onset. With the cue offset, the participants had to report the detection of a tactile stimulus (yes/no). After the yes/no-button press, a pause screen was displayed for 0.3 s, before the participants were asked to report their decision confidence (confident/unconfident). With pressing the

button for “confident” or “unconfident”, the new trial started. For both reports, the maximum response time was 1.5 s. Thus, the trial duration was limited to 5.8 s.

Participants indicated their perception and decision confidence with the right index finger on a two-button box. The buttons were arranged vertically. The four possible button response mappings were counterbalanced across participants, so that the top button could be assigned to “yes” or “no”, and “confident” or “unconfident” respectively for one participant.

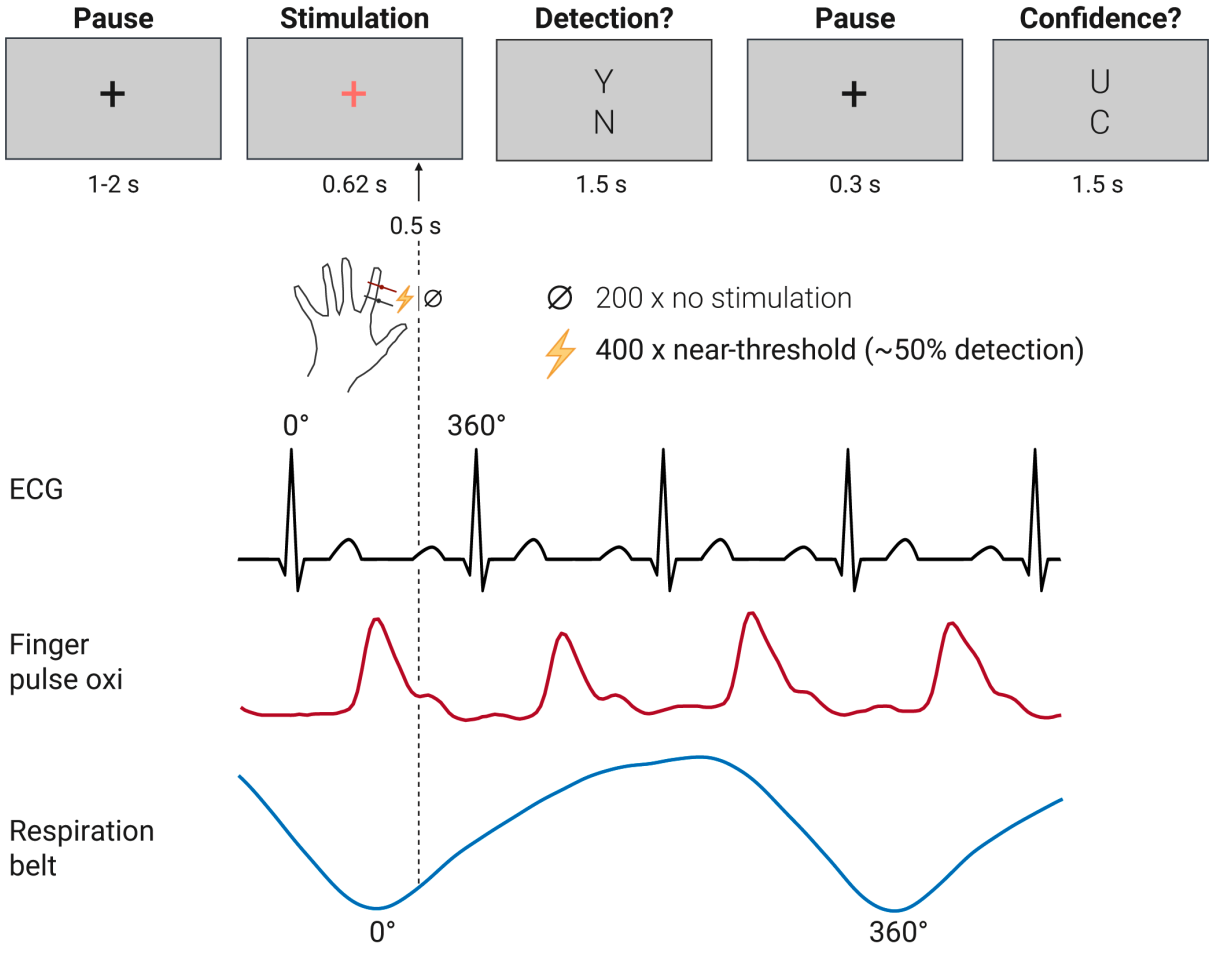

Figure 1. Experimental procedure and physiological parameters visualized for one exemplary trial. The tiles represent the participant’s visual display and the times given below indicate the presentation duration. The near-threshold electrical finger nerve stimulation was always 0.5 s after the cue onset (salmon-colored fixation cross). Here only one of four button response mappings is displayed (Y = yes; N = no; U = unconfident; C = confident). In total, 400 near-threshold trials and 200 trials without

stimulation (33% catch trials) were presented in a randomized order. Exemplary traces of electrocardiogram (ECG), finger pulse oximetry, and respiration belt below the trial procedure indicate that stimulus detection was analyzed relative to cardiac and respiratory cycles (0-360°).

Prior to the experiment, participants were familiarized with the electrical finger nerve stimulation and an automatic threshold assessment was performed in order to determine the stimulus intensity corresponding to the sensory threshold (50% detection rate). The threshold assessment entailed an up-and-down procedure followed by a Bayesian approach (psi method) from the Palamedes Toolbox (Kingdom and Prins, 2009) and closed with a test block. The visual display of the trials in the threshold assessment was similar to the trials in the experimental block (Figure 1) but without the confidence rating and a shorter fixed intertrial interval (0.5 s). If necessary, the threshold assessment was repeated before each block to ensure a detection rate of 50% throughout the whole experiment. The experimental procedure was controlled by custom MATLAB scripts using the Psychophysics Toolbox (Kleiner et al., 2007).

Electrocardiogram acquisition

The electrocardiogram (ECG) was recorded with the BrainAmp ExG (Brain Products, Gilching, Germany) between two adhesive electrodes that were placed on the sternum and just below the heart on the left side of the thorax. A ground electrode was placed on the acromion of the right shoulder. The sampling frequency was 5000 Hz for 39 participants. Two participants were recorded with 1000 Hz.

227 **Respiration acquisition**

228 Respiration was measured with a respiration belt (BrainAmp ExG; Brain Products,
229 Gilching, Germany). The belt with a pressure-sensitive cushion was placed at the
230 largest expansion of the abdomen during inspiration. The sampling frequency was
231 5000 Hz for 39 participants. Two participants were recorded with 1000 Hz.

232

233 **Peripheral nerve activity acquisition**

234 To examine the possibility to measure somatosensory evoked potentials (SEP) of
235 peripheral nerve activity in response to near-threshold finger stimulation, two surface
236 electrodes were placed with a distance of 2 cm at the left upper inner arm (below the
237 biceps brachii) above the pathway of the median nerve in a sub-sample of 12
238 participants. The signal was recorded with a sampling rate of 5000 Hz, low-pass
239 filtered at 1000 Hz, using a bipolar electrode montage (BrainAmp ExG; Brain
240 Products, Gilching, Germany).

241

242 **Oximetry acquisition**

243 The pulse oximetry was recorded with a finger clip SpO_2 transducer at the left middle
244 finger at 50 Hz (OXI100C and MP150; BIOPAC Systems Inc., Goleta, California, USA).

245

246 **Behavioral data analysis**

247 The behavioral data was analyzed with R 4.0.3 in RStudio 1.3.10923. First, trials were
248 filtered for detection and confidence responses within the maximum response time
249 of 1.5 s. Second, only blocks were considered with a near-threshold hit rate at least
250 five percentage points above the false alarm rate. These resulted in 37 participants

with 4 valid blocks, 2 participants with 3 valid blocks and 2 participants with 2 valid blocks. The frequencies of the response "confident" for correct rejections, misses, and hits were compared with paired *t*-tests. Furthermore, the detection and confidence response times and resulting trial durations were compared between correct rejections, misses, and hits with paired *t*-tests. The response times for hits and miss were additionally compared between confident and unconfident near-threshold trials.

Cardiac data analysis

ECG data was preprocessed with Kubios (Version 2.2) to detect R-peaks. For two participants, the first four and the first twenty-two trials respectively had to be excluded due to a delayed start of the ECG recording. Additionally, one block of one participant and two blocks of another participant were excluded due to low ECG data quality.

First for correct rejections, misses, and hits, the circular distribution within the cardiac cycle was assessed with the Rayleigh test of uniformity. Additionally, this analysis was repeated for confident and unconfident hits and misses.

Second, instead of the relative position within the cardiac cycle, near-threshold trials were assigned to four time intervals based on their temporal distance from the previous R-peak (0-200 ms, 200-400 ms, 400-600 ms, and 600-900 ms). The last interval had a duration of 300 ms to account for interindividual differences of the interbeat interval and aggregate a similar number of trials to the preceding intervals. Then, detection rates for confident and unconfident decisions were calculated in each

time interval and compared with a two-way repeated measures ANOVA and post-hoc *t*-tests.

Third, we analyzed the interbeat intervals in the course of a trial between the stimulus-response conditions. For this, two interbeat intervals before, one during, and two after the stimulus onset were selected and compared with a two-way repeated measures ANOVA and post-hoc *t*-tests.

Oximetry data analysis

Oximetry data was analyzed with custom MATLAB scripts to detect the pulse wave peaks with a minimum peak distance based on 140 heartbeats per minute and a minimum peak prominence equal to a tenth of the data range in each block. Pulse cycles with a duration 1.5 times the median duration of the respective block were excluded from further processing. In R, the pulse wave cycle data was merged with the behavioral data to apply the same exclusion criteria and the Rayleigh test of uniformity. Finally, pulse wave peaks were located in the cardiac cycle to assess the duration since the previous R-peak (pulse wave transit time, PWTT) and its relative position in degree within the cardiac cycle.

Respiration data analysis

After visual inspection of the respiration traces, respiratory cycle detection was performed following the procedure by Power et al. (2020). First, outliers were replaced in a moving 1-s window with linearly interpolated values based on neighboring, non-outlier values. Local outliers were defined as values of more than three local scaled median absolute deviations (MAD) away from the local median within a 1-s window

(Power et al., 2020). MAD was chosen for its robustness compared to standard deviation which is more affected by extreme values. Subsequently, the data was smoothed with a 1-s window Savitzky-Golay filter (Savitzky and Golay, 1964) to facilitate peak detection. Traces were then z-scored and inverted to identify local minima (inspiration onsets) with the MATLAB findpeaks function. Local minima had to be at least 2 s apart with a minimum prominence of 0.9 times the interquartile range of the z-scored data. Respiration cycles were defined as the interval from one inspiration onset to the next inspiration onset. For each participant, respiration cycles with more than two times the median cycle duration were excluded from further analysis.

For each stimulus-response condition and participant, the mean angle direction of stimulus onsets within the respiration cycle and their circular variance across trials were calculated. The distribution of mean angles of each stimulus-response condition was tested for uniformity with the Rayleigh test. Circular variance was defined as $V = 1\text{-}R$, where R is the mean resultant length of each stimulus-response condition and participant with values between 0 and 1. Differences in circular variances between stimulus-response conditions were assessed with paired *t*-tests.

Furthermore, we investigated whether participants gradually aligned their respiration to the stimulus onset in the beginning of the experiment. For the first 30 trials, the difference between each trial's stimulus onset angle and the mean angle within the first block was determined ("diff_angle2mean"). The trial angle difference from the mean was used as a dependent variable in a random-intercept linear regression based on maximum likelihood estimation with trial number as independent

variable: "diff_angle2mean ~ 1 + trial + (1|participant)". The fit of this model was compared with a random-intercept only model "diff_angle2mean ~ 1 + (1|participant)" in a χ^2-test to assess the effect of trial number on the angle difference. This analysis included only the 37 participants with a valid first block and excluded trials with false alarms.

Lastly, we compared the respiratory cycle duration between stimulus-response conditions by performing a one-way repeated-measures ANOVA and post-hoc *t*-tests.

Phase-locking analysis between cardiac and respiratory activity

The n:m ($n, m \in N$) synchronization (Lachaux et al., 1999) was calculated in an inter-trial setting for the stimulation onset as the following:

$$PLV_{cross} = \left| \frac{1}{n} \sum_{i=1}^{n} e^{j\phi_i} \right|$$

$$\phi_i = n\,\Phi_{i,resp} - m\,\Phi_{i,ecg}$$

where $\Phi_{i,resp}$ and $\Phi_{i,ecg}$ were the stimulation onset angles for the i-th trial within the respiratory (*resp*) and cardiac cycle (*ecg*), and *j* was the imaginary number. While $m = 1$ was chosen for all participants, values for n were selected by calculating the ratio of the cardiac and respiratory frequency rounded to the nearest integer. The frequencies were estimated based on the mean cardiac and respiratory cycle durations at stimulus onset. The inter-trial n:m synchronization at stimulation onset can provide information about the extent to which the weighted phase difference of the two signals stays identical over trials. The calculated phase-locking value (PLV) lies between zero and one, with zero indicating no inter-trial coupling and one showing a constant weighted phase-difference of the two signals at the stimulation time.

346 **Somatosensory evoked potential analysis**

347 For the twelve participants with peripheral nerve recordings, stimulation artefacts
348 were removed with a cubic monotonous Hermite spline interpolation from -2 s until 4
349 s relative to the trigger. Next, a 70-Hz high-pass filter was applied (4th order
350 Butterworth filter applied forwards and backwards) and the data was epoched -100
351 ms to 100 ms relative to the trigger with -50 ms to -2 ms as baseline correction.
352 Subsequently, epochs were averaged across for valid trials (yes/no and confidence
353 response within maximum response time) with near-threshold stimuli and without
354 stimulations.

Results

Detection and confidence responses

Participants (N = 41) detected on average 51% of near-threshold stimuli (SD = 16%) and correctly rejected 94% of catch trials without stimulation (SD = 6%). On average, 188 catch trials (range: 93-200) and 375 near-threshold trials (range: 191-400) were observed. Participants reported to be "confident" about their yes/no-decision in 88% of the correct rejections (SD = 13%), in 71% of the misses (SD = 21%), and in 62% of the hits (SD = 18%). The confidence rate differed significantly between all conditions in paired t-tests (CR vs. miss: $p = 3 * 10^{-8}$; CR vs. hit: $p = 1 * 10^{-9}$; miss vs. hit: p = 0.019). In total, we observed on average 184 misses (range: 58-303), 192 hits (range: 59-302), 177 correct rejections (range: 72-198) and 11 false alarms (range: 0-36). Two-third of the participants (27) had less than ten false alarms and four participants had zero false alarms. Due to zero or very few observations, false alarms were not further analyzed.

In near-threshold trials, participants reported their yes/no-decision later than for correct rejections (mean ± SD: RT_{Hit} = 641±12 ms, RT_{Miss} = 647±12 ms, RT_{CR} = 594±10 ms; paired t-test hit vs. CR: p = 0.02, miss vs. CR: $p = 3 * 10^{-8}$). The yes/no-response times for hits and misses did not differ significantly (p = 0.43). Additionally in unconfident compared to confident near-threshold trials, yes/no-responses were on average 221 ms slower (mean ± SD: RT_{Near_unconf} = 789±11 ms, RT_{Near_conf} = 569±9 ms; paired t-test: $p = 2 * 10^{-16}$). Splitting near-threshold trials by confidence resulted in on average 49 unconfident misses (range: 6-143), 135 confident misses (range: 29-289), 70 unconfident hits (range: 9-181), and 122 confident hits (range: 24-277).

Cardiac cycle

First, we addressed the question whether stimulus detection differed along the cardiac cycle. For hits, mean angles within the cardiac cycle were not uniformly distributed ($R = 0.34$, $p = 0.007$; Figure 2), indicating a relation between cardiac phase and stimulus detection. Sixteen participants had a mean angle for hits in the last quarter of the cardiac cycle (270-360°). The Rayleigh tests were not significant for misses ($R = 0.20$, $p = 0.18$) and correct rejections ($R = 0.05$, $p = 0.91$).

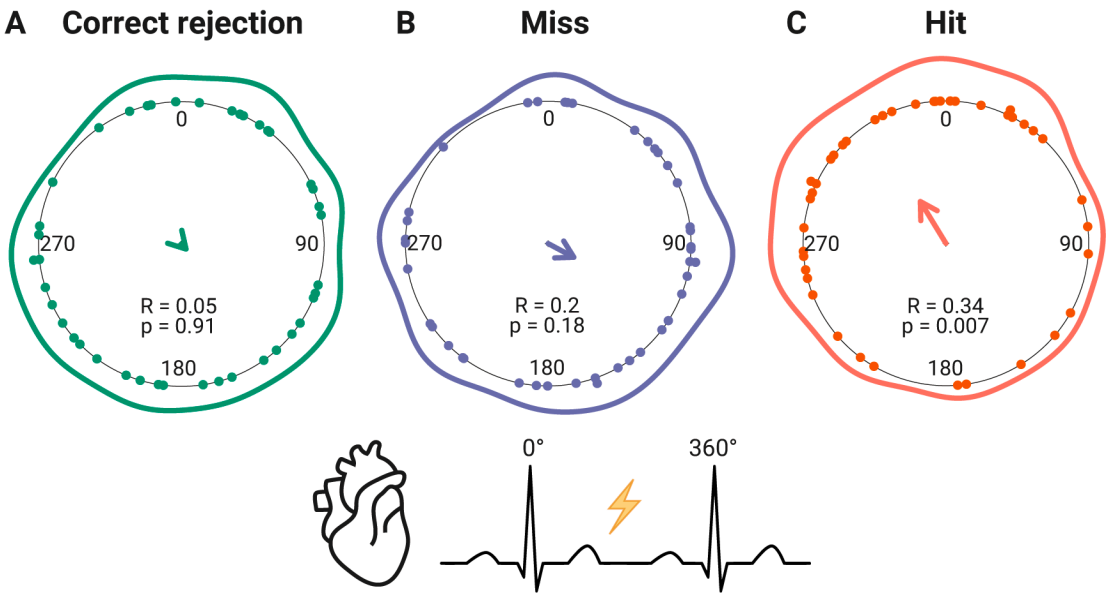

Figure 2. Distribution of mean angles (stimulus onset relative to cardiac cycle) for (***A***) correct rejections (green), (***B***) misses (purple), and (***C***) hits (red). Each dot indicates a mean angle by one participant. The line around the inner circle shows the density distribution of these mean angles. The direction of the arrow in the center indicates the mean angle across the participants while the arrow length represents the mean resultant length *R*. The resulting p-value of the Rayleigh test of uniformity is noted below.

Second, we repeated the analysis by splitting near-threshold trials based on the reported decision confidence. The unimodal distribution was also present for confident hits ($R = 0.38$, $p = 0.002$) but not for unconfident hits ($R = 0.10$, $p = 0.69$). Eighteen participants had a mean angle for confident hits in the last quarter of the

cardiac cycle (270-360°). Confident misses also showed a unimodal distribution (R = 0.28, p = 0.04). Unconfident misses (R = 0.22, p = 0.14), confident correct rejections (R = 0.005 p = 1.00) and unconfident correct rejections (R = 0.01, p = 1.00) did not allow to reject the uniform distribution. Two participants were excluded from the analysis of unconfident correct rejections due to zero unconfident correct rejections (mean n = 20, SD = 22, range: 0-88).

Third, near-threshold detection was analyzed separately for confident and unconfident decisions within four time intervals after the R-peak (0-200 ms, 200-400 ms, 400-600 ms, 600-900 ms). First, we calculated a two-way repeated measures ANOVA with near-threshold detection rate as dependent variable and time interval and decision confidence as within-participants factors. The ANOVA showed a main effect between confidence categories (F(1,40) = 7.84, p = 0.008) and an interaction effect of time and confidence categories on near-threshold detection (F(3,120) = 3.09, p = 0.03). Subsequently, post-hoc t-tests were calculated between confidence categories for each time interval and between time intervals within each confidence category (Figure 3). The detection rate was significantly lower for confident compared to unconfident decisions within the first two time intervals (0-200 ms: FDR-corrected p = 0.02; 200-400 ms: FDR-corrected p = 0.02). Between time intervals, we only observed for confident decisions a significant lower detection rate at 200-400 ms compared to 400-600 ms (FDR-corrected p = 0.02) and 600-900 ms (FDR-corrected p = 0.02).

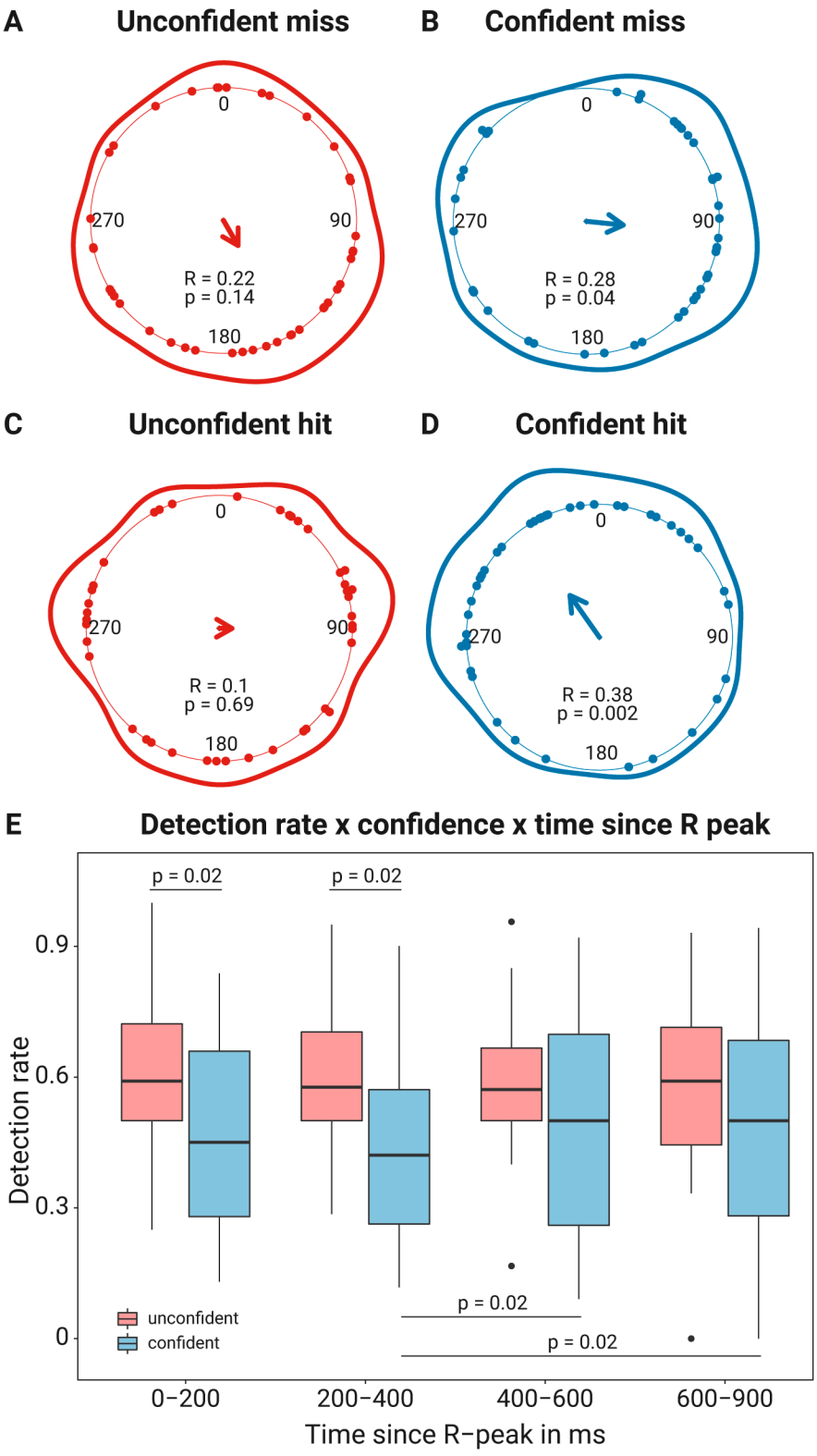

Figure 3. Circular distribution within the cardiac cycle of unconfident/confident misses and hits (***A-D***) and detection rates for unconfident and confident decisions at four time intervals after the R-peak (***E***). The distributions of mean angles (stimulus onset relative to cardiac cycle) are shown for (***A***) unconfident misses (red), (***B***) confident misses (blue), (***C***) unconfident hits (red), and (***D***) confident hits (red). In ***A-D***,

each dot indicates a mean angle by one participant. The line around the inner circle shows the density distribution of these mean angles. The direction of the arrow in the center indicates the mean angle across the participants while the arrow length represents the mean resultant length *R*. The resulting p-value of the Rayleigh test of uniformity is noted below. ***E***, Boxplots show the distribution of detection rates for unconfident (red) and confident (blue) decisions at four time intervals after the R-peak. Boxplots indicate the median (centered line), the 25%/75% percentiles (box), 1.5 times the interquartile range or the maximum value if smaller (whiskers), and outliers (dots beyond the whisker range). Significant post-hoc *t*-tests are indicated with a black bar and the respective FDR-corrected *p*-value.

Cardiac interbeat interval

For each stimulus-response condition (hit, miss, and correct rejection), we extracted the interbeat interval entailing the stimulus onset, as well as the two preceding and subsequent interbeat intervals (Figure 4A). We used a two-way repeated measures ANOVA to test the factors time and stimulus-response condition, and their interaction on interbeat intervals. The main effect of time ($F(2.73,109.36) = 35.60$, $p = 3 \times 10^{-15}$) and the interaction of time and stimulus-response condition ($F(4.89,195.55) = 4.92$, $p = 0.0003$) were significant. There was no significant main effect of stimulus-response condition on interbeat intervals ($F(1.42,56.75) = 2.35$, $p = 0.12$). Following, post-hoc *t*-tests were calculated at each interbeat interval between the stimulus-response conditions (5 x 3) and within each stimulus-response condition between subsequent interbeat intervals (3 x 4), resulting in 27 FDR-corrected *p*-values. At “S+1”, the interbeat intervals (IBI) for hits were significantly longer than for misses ($\Delta IBI = 5.2$ ms, FDR-corrected $p = 0.024$) and correct rejections ($\Delta IBI = 4.4$ ms, FDR-corrected $p = 0.017$). The interbeat intervals between misses and correct rejections did not differ significantly (FDR-corrected $p = 0.62$). At “S+2”, the interbeat intervals for hits were still longer compared to correct rejections ($\Delta IBI = 5.3$ ms, FDR-corrected $p = 0.014$)

but not to misses (FDR-corrected $p = 0.25$). Within each stimulus-response condition (hit, miss, and correct rejection) subsequent interbeat intervals differed significantly (FDR-corrected $p < 0.005$).

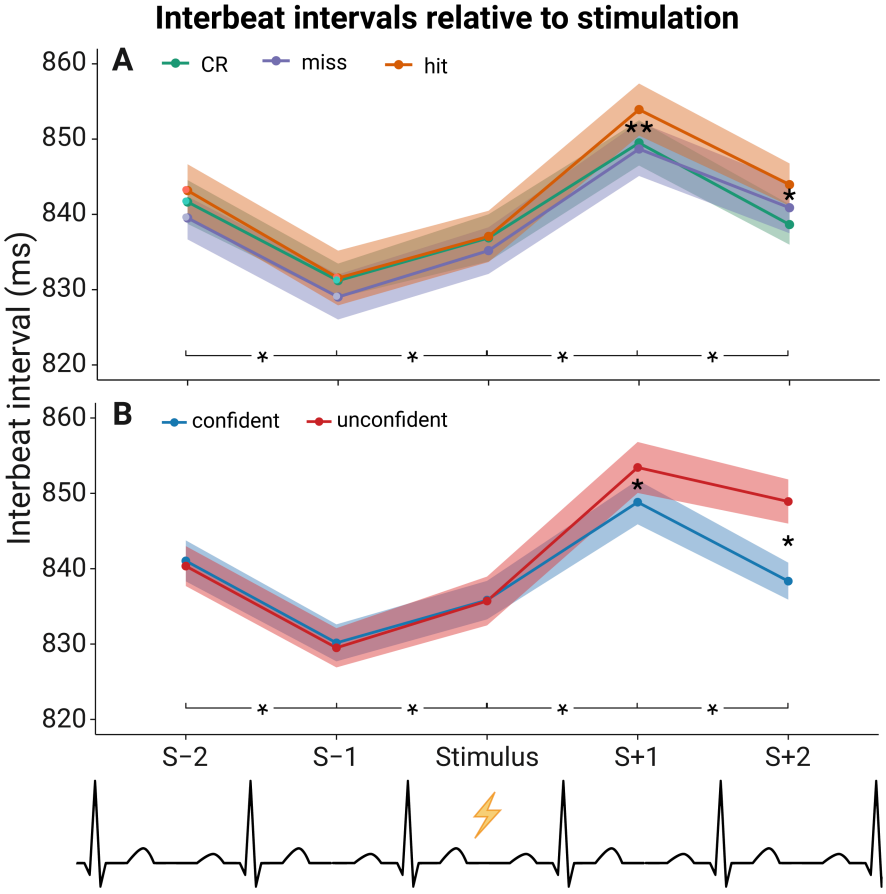

Figure 4. Interbeat intervals before and after the stimulus onset for (***A***) correct rejections (green), misses (purple), and hits (red), and for (***B***) confident (blue) and unconfident (red) decisions. Confidence bands reflect within-participant 95% confidence intervals. The label "Stimulus" on the y-axis indicates the cardiac cycle when the stimulation or cue only were present. The labels "S-1" and "S+1" indicate the preceding and following intervals respectively. In ***A***, the two asterisks "**" at "S+1" indicate significant FDR-corrected *t*-tests between hits and misses, and between hits and correct rejections. The one asterisk "*" at "S+2" in ***A*** indicates a significant FDR-corrected *t*-test between hits and correct rejections. In ***B***, the asterisks at "S+1" and "S+2" indicate significant FDR-corrected *t*-tests between confident and unconfident decisions. The lines with asterisks on the bottom indicate significant FDR-corrected *t*-tests for subsequent interbeat intervals within all conditions.

Furthermore, interbeat intervals of trials with confident and unconfident decisions independent of stimulus presence and yes/no-response (excluding false alarms) were compared with a two-way repeated measures ANOVA (Figure 4B). The main effects time ($F(2.71, 108.31) = 42.37$, $p = 2 \times 10^{-16}$) and confidence ($F(1,40) = 5.36$, $p = 0.026$), as well as the interaction of time and confidence were significant ($F(2.73, 109.05) = 30.79$, $p = 2 \times 10^{-16}$). Post-hoc *t*-tests between the two confidence categories for each interbeat interval (1 x 5) and within each confidence category between subsequent interbeat intervals (2 x 4) revealed significant longer post-stimulus interbeat intervals for unconfident compared to confident decisions at "S+1" (ΔIBI = 4.6 ms, FDR-corrected p = 0.005) and "S+2" (ΔIBI = 10.6 ms, FDR-corrected $p = 6 \times 10^{-7}$). All subsequent interbeat intervals differed significantly within each confidence category (FDR-corrected $p < 0.05$). When repeated for near-threshold trials only, the difference between confidence categories was still present within each awareness condition: unconfident hits and misses showed longer interbeat intervals at "S+2" compared to confident hits (ΔIBI = 5.7 ms, FDR-corrected p = 0.047) and confident misses respectively (ΔIBI = 10.2 ms, FDR-corrected p = 0.008).

Pulse wave relative to electric cardiac cycle

Next to the electric cardiac cycle, we assessed whether stimulus detection was dependent on the pulse wave cycle measured at the left middle finger. Pulse wave peaks were located in the cardiac cycle by calculating the time to the preceding R-peak: the pulse wave transit time (PWTT) and the PWTT relative to its current cardiac cycle in degree. The PWTT was on average 405 ms (SD = 24 ms, range: 354-439 ms). The pulse wave peak occurred on average in the middle of the cardiac cycle (mean

angle M_{PWTT} = 178°, R = 0.91, p = 0) after the mean angle of confident misses ($M_{Confident\ miss}$ = 96°) and before the mean angle of confident hits ($M_{Confident\ hit}$ = 325°).

For putting the observed correlations between detection and the cardiac cycle in relation to the pulse wave peak, the analysis of near-threshold hit rates during different stimulus onset intervals after the R-peak was repeated limited to 0-400 ms with shorter intervals (50 ms) and without splitting by confidence. A one-way repeated-measures ANOVA showed a main effect by time interval on near-threshold detection rate (F(5.64, 225.46) = 3.15, p = 0.007). The near-threshold hit rates were significantly decreased before the pulse wave peak (mean PWTT = 405 ms) during the interval of 250-300 ms compared to the interval of 0-50 ms (FDR-corrected p = 0.038). The interval 250-300 ms was plotted on the average pulse wave locked to the preceding R-peak and its slope (difference between adjacent samples). It shows that after 250 ms the pulse wave substantially increases (Figure 5B).

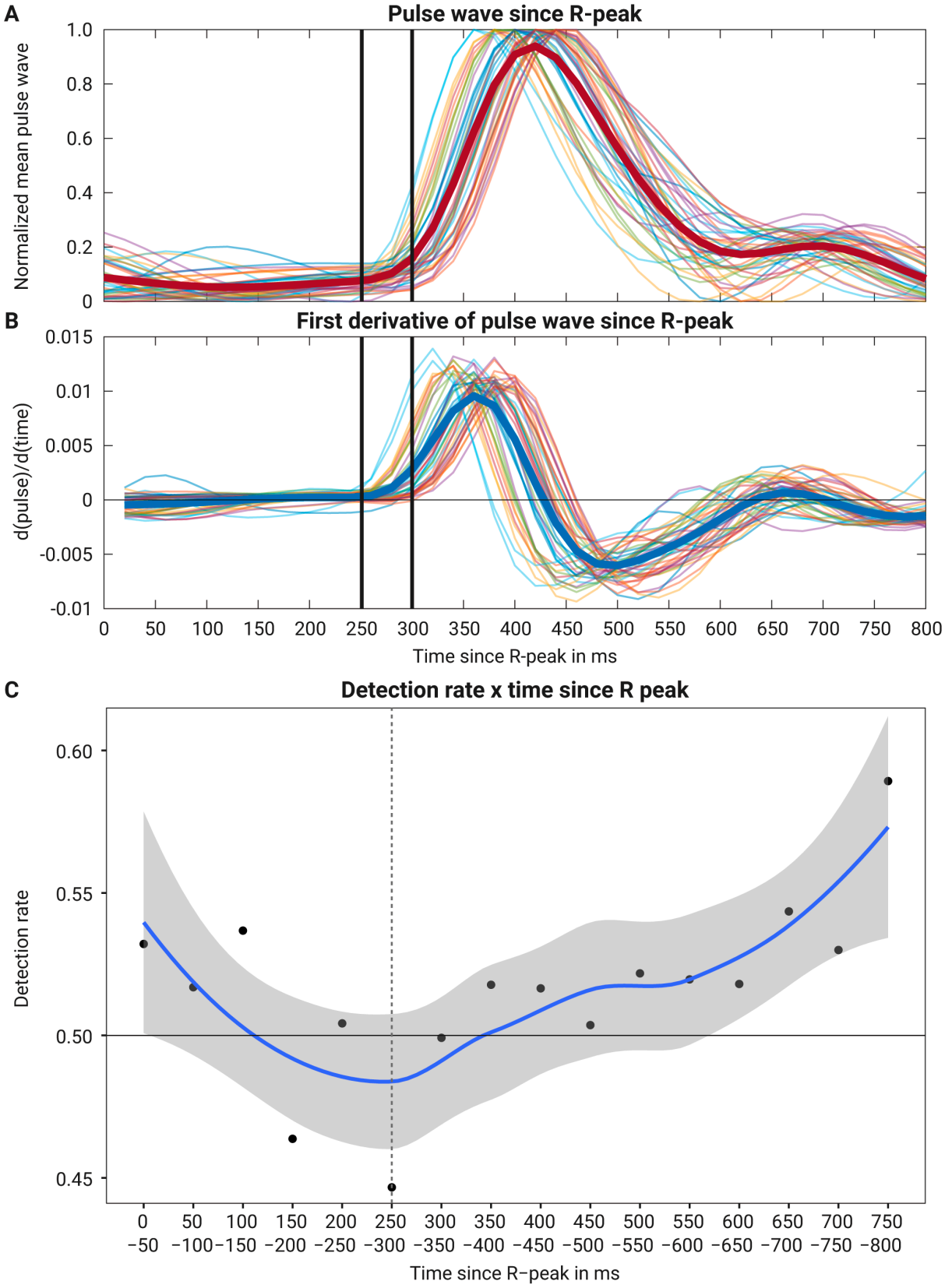

Figure 5. Pulse wave and detection relative to cardiac cycle. (***A***) Mean pulse wave measured at the left middle finger for each participant locked to preceding R-peak. (***B***) First derivative of the mean pulse wave. (***C***) Detection rate of near-threshold trials in 50-ms stimulus onset intervals since preceding R-

peak. The black dots indicate the mean across participants. The blue line is the locally smoothed loess curve with a 95% confidence interval (grey) across these means.

Respiratory cycle

First, we investigated whether conscious tactile perception depends on the stimulus onset relative to the respiratory cycle. Thus, we calculated the mean angles for hits, misses, and correct rejections for each participant and tested their circular distribution with the Rayleigh test of uniformity. For all conditions, uniformity was rejected in favor of an alternative unimodal distribution (correct rejections: $R = 0.58$, $p = 4 \times 10^{-7}$; misses: $R = 0.54$, $p = 2 \times 10^{-6}$; hits: $R = 0.65$, $p = 1 \times 10^{-8}$; Figure 6). These unimodal distributions were centered at stimulus onset for the three conditions (mean angle $M_{\text{correct rejection}} = 3.2°$, $M_{\text{miss}} = 5.0°$, and $M_{\text{hit}} = 15.1°$). To assess whether the strength of the inhale onset locking differed significantly between hits, misses, and correction rejections, the circular variance of stimulus onset angles across trials was calculated for each stimulus-response condition and compared with *t*-tests. Hits had a lower circular variance than misses ($\Delta V = -0.044$, $t(40) = -3.17$, $p = 0.003$) and correct rejections ($\Delta V = -0.035$, $t(40) = -2.78$, $p = 0.008$), i.e., exhibited a stronger clustering around the mean direction . There was no significant difference in circular variance between misses and correct rejections ($p = 0.44$). Additionally, we investigated whether the detection rate of near-threshold trials varied across the cardiac cycle. For this purpose, near-threshold trials were assigned to four subsequent 1-s time intervals relative to the preceding inhale onset (0-4 s). A one-way repeated-measures ANOVA could not establish an effect by time interval on near-threshold detection rate ($F(1.81,72.30) = 0.83$, $p = 0.43$).

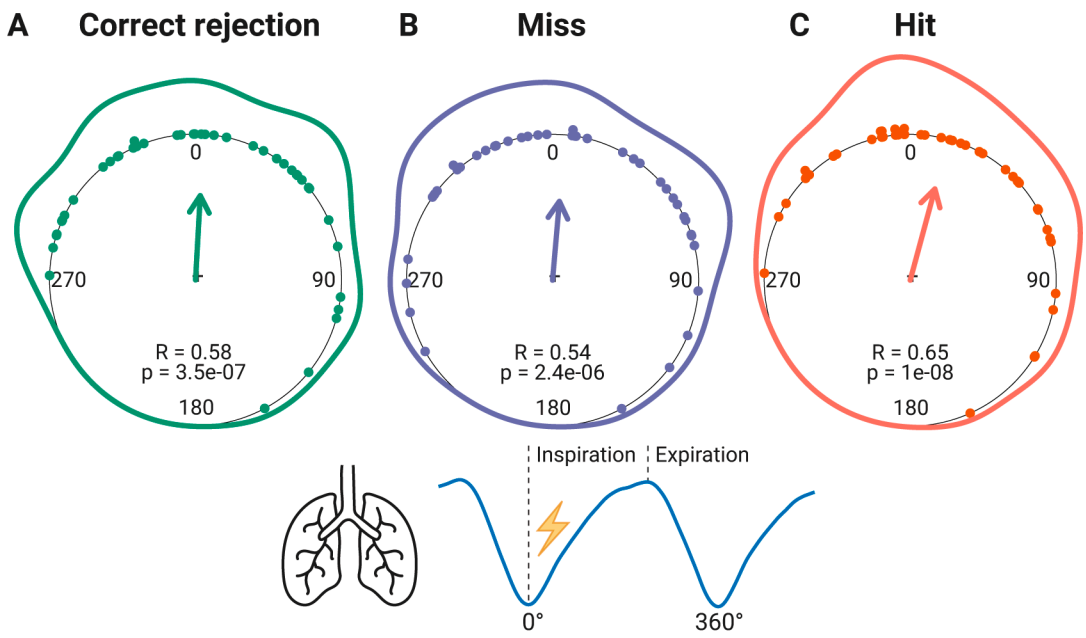

Figure 6. Circular distribution of mean stimulus onsets relative to the respiratory cycle for (***A***) correct rejections (green), (***B***) misses (purple), and (***C***) hits (red). Zero degree indicates the inspiration onset. Each dot indicates a mean angle by one participant. The line around the inner circle shows the density distribution of these mean angles. The direction of the arrow in the center indicates the mean angle across the participants while the arrow length represents the mean resultant length *R*. The resulting p-value of the Rayleigh test of uniformity is noted below.

Second, the distribution of mean angles was assessed for confident and unconfident decisions. Hits, misses, and correct rejections were split by decision confidence and the resulting distributions were evaluated with the Rayleigh test for uniformity. All stimulus-response conditions showed for unconfident and confident decisions a significant unimodal distribution locked around the stimulus onset: unconfident correct rejections (mean angle M_{unconf_CR} = 18.3°; R = 0.41, p = 0.001), confident correct rejections (M_{conf_CR} = 2.2°; R = 0.58, p = 4 x 10^{-7}), unconfident misses (M_{unconf_miss} = 13.4°; R = 0.45, p = 0.0001), confident misses (M_{conf_miss} = 6.7°, R = 0.51; p = 0.00001), unconfident hits (M_{unconf_hit} = 10.4°; R = 0.51, p = 0.0001), and confident

hits (M_{conf_hit} = 15.2°; R = 0.67, p = 4 x 10^{-9}). Two participants had zero unconfident correct rejections and were not considered in the respective Rayleigh test.

Third, in order to examine aforementioned phase effects further, we investigated whether participants adjusted their respiration rhythm to the paradigm in the beginning of the experiment. Thus for the first 30 trials of the first block, a random-intercept linear regression model with maximum likelihood estimation (lmer function in R) was calculated to evaluate the effect of trial number on trial angle difference from the mean for each participant. The angle difference was determined between the stimulus onset angle within the respiratory cycle of each trial and the mean of all angles in the first block ("diff_angle2mean"). This analysis included 37 participants with a first block and excluded trials with false alarms. Comparing the model "diff_angle2mean ~ 1 + trial + (1|participant)" with a random intercept-only model "diff_angle2mean ~ 1 + (1|participant)" revealed an effect of trial on the difference to the angle mean within the first 30 trials of the first block (χ^2 = 5.84, p = 0.016). The fixed-effect slope was b_1 = -0.47 and the mean of the random-intercepts b_0 = 79.7 (*diff_angle2mean* = b_1 * *trial* + b_0).

Respiratory cycle duration

Given the previously reported heart slowing during conscious tactile perception (Motyka et al., 2019)., we tested whether a similar effect was also present in the respiratory rhythm. Indeed, the mean duration of respiratory cycles differed between response categories (Figure 7), as indicated by a one-way repeated-measures ANOVA (F(1.49, 59.61) = 13.11, p = 0.0001). Post-hoc t-tests showed that respiratory cycles accompanying misses (mean t = 3.86 s) were significantly longer than

568 respiratory cycles with correct rejections (mean t = 3.82 s, Δt = 40 ms, FDR-corrected
569 p = 0.002) and with hits (mean t = 3.77 s, Δt = 91 ms, FDR-corrected p = 0.0002).
570 Respiratory cycles with hits were also significantly shorter than correct rejections (Δt
571 = 50 ms, FDR-corrected p = 0.014).

572 Additionally, we analyzed whether the respiratory cycle duration differed
573 between confident and unconfident hits and misses. There was a main effect by
574 detection (F(1, 40) = 14.64, p = 0.0004) but not by confidence (F(1, 40) = 1.15, p =
575 0.29) on respiratory cycle duration in a two-way repeated measures ANOVA. The
576 interaction of detection and confidence was not significant (F(1, 40) = 0.83, p = 0.37).

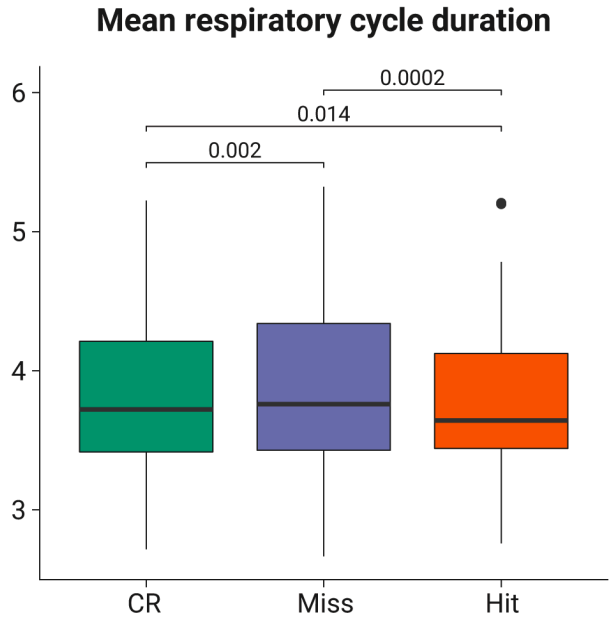

577

578 **Figure 7.** Mean respiratory cycle duration in seconds for correct rejections (green), misses (purple),
579 and hits (red). The boxplots indicate the median (centered line), the 25%/75% percentiles (box), 1.5
580 times the interquartile range or the maximum value if smaller (whiskers), and outliers (dots beyond the
581 whisker range). Significant post-hoc t-tests are indicated above the boxplot with a black bar and the
582 respective FDR-corrected p-value.

583 **Phase-locking between cardiac and respiratory activity**

584 Due to the natural coupling of cardiac and respiratory rhythms (Dick et al., 2014), we
585 investigated whether phase-locking of both rhythms is associated with conscious
586 tactile perception. Phase-locking values (PLVs) were calculated across trials using
587 n:m synchronization (Tass et al., 1998; Lachaux et al., 1999) to account for the
588 different frequency bands of the two signals. PLVs were compared between hits,
589 misses, and correct rejections with a one-way repeated-measures ANOVA. The
590 ANOVA showed no significant main effect of stimulus-response condition on PLVs
591 between cardiac and respiratory activity ($F(1.98,79.15) = 1.72$, $p = 0.19$).

592

593 **Peripheral nerve activity**

594 For the sub-sample of twelve participants with peripheral nerve recordings at the left
595 upper arm, there was no somatosensory evoked potential associated with near-
596 threshold stimuli. Also, the grand mean across participants did not show a difference
597 between trials with and without near-threshold stimulation. We concluded that near-
598 threshold stimulation intensities (in the given sub-sample on average 1.88 mA, range:
599 0.79-2.50 mA) did not produce sufficiently high peripheral somatosensory evoked
600 potentials to measure them non-invasively from the inner side of the upper arm.
601 Hence, we did not further pursue the analysis of peripheral somatosensory evoked
602 potentials. (Yet note that peripheral somatosensory evoked potentials were observed
603 in a pilot study with the same acquisition setup but applying super-threshold
604 stimulation intensities of 6 mA.)

Discussion

In a tactile detection paradigm with near-threshold electrical finger nerve stimulation, cardiac and respiratory activity was observed with electrocardiography (ECG), pulse oximetry, and a respiration chest belt. The present study is the third independent study, where we observed a cardiac cycle effect on tactile detection (hits more likely during diastole) and a pronounced heart slowing with conscious tactile perception (Motyka et al., 2019; Al et al., 2020). The previously reported lower tactile detection during systole (Al et al., 2020) and the unimodal distribution of hits in diastole (Motyka et al., 2019; Al et al., 2020) were both only present when decision confidence was high. Using finger pulse oximetry, we identified that the lowest tactile detection rate between 250 and 300 ms after the R-peak corresponded to the pulse wave onset. We furthermore showed that the respiration rhythm adapted to the tactile detection paradigm, such that inhale onsets tended to be locked to expected stimulus onsets. This locking of inhale onsets to stimulus onset was more consistent for detected compared to undetected near-threshold trials. Respiratory cycles accompanying misses were longer in comparison to hits and correct rejections.

Detection varies across the cardiac cycle only for confident decisions

Relating tactile detection to cardiac activity revealed that hits were not uniformly distributed across the cardiac cycle and more likely to appear in the last quarter, as we have shown previously (Motyka et al., 2019; Al et al., 2020). Splitting hits and misses by decision confidence - not possible in our previous studies - showed that this unimodal distribution was only present for confident but not unconfident hits.

Additionally, also confident but not unconfident misses showed a unimodal distribution (centered around 90 degrees).

When we analyzed the near-threshold detection rate for four stimulus onset intervals relative to the preceding R-peak split by decision confidence, we observed that detection was lower when the decision was confident. Furthermore, only confident hits were reduced in the second time interval (200-400 ms) compared to the two later timer intervals (400-900 ms). In our previous study (Al et al., 2020), a decreased detection rate was observed for the very same time interval.

While replicating the unimodal distribution of hits within the cardiac cycle here for the third time in an independent study of somatosensory detection (Motyka et al., 2019; Al et al., 2020), the explanation for this effect still stays speculative. It seems highly plausible that the decreased detection rate between 200 and 400 ms after the R-peak is related to the arrival of the pulse wave in the finger at circa 250 ms or heartbeat sensations (see below discussion on *Pulse wave*). Our finding that the number of confident hits is reduced (in contrast to unconfident ratings) seems consistent with a “late” event in the perceptual decision-making process. This is in line with our previous EEG study which has shown that only late cortical somatosensory evoked potentials (P300) are increased for stimuli during diastole compared to systole (Al et al., 2020). Hence, both, the reduction of confident hits and the modulation of (only) late SEP-components, speak for higher cognitive processes as meta-cognition or prediction to be involved in the cardiac cycle effect on conscious tactile perception.

Pulse wave onset marks decreased detection in cardiac cycle

Addressing the hypothesis whether decreased near-threshold detection 200-400 ms after the R-peak was caused by the pulse wave peak in the finger (Al et al., 2020), pulse wave peaks were located in the cardiac cycle. As a result, the decreased near-threshold detection rate was located more precisely 250-300 ms after the R-peak, before the pulse wave peak (405 ms) in the middle of the cardiac cycle (178°). Inspecting the slope of the pulse wave showed a take-off around 250 ms after the preceding R-peak, indicating the pulse wave onset.

If a suppressive top-down mechanism for pulse wave related changes in the finger affects near-threshold tactile detection, then it might be already sensitive to initial changes of the pulse wave in the finger than only to its peak (Macefield, 2003). Perception of heartbeats has been reported to occur in the very same time interval of 200-300 ms after the R-peak (Yates et al., 1985; Brener and Kluvitse, 1988; Ring and Brener, 1992). While this temporal judgement is unlikely to be solely based on the pulse wave in the finger - heartbeat sensations were mainly localized on the chest (Khalsa et al., 2009; Hassanpour et al., 2016), it might be possible that the prediction of strongest heartbeat-related changes at 250-300 ms attenuated the detection of weak stimuli presented in the same time window. Temporally locating the lower tactile detection during systole at the pulse wave onset in the finger provides further evidence for the view that the cardiac cycle effect does not correspond to maximal peripheral cardiac changes. It rather suggests that this is a conflict on the perceptual level during an interval with the highest uncertainty whether a weak pulse was generated internally (heartbeat) or applied externally (Allen et al., n.d.).

673 **Heart slowing with conscious perception and unconfident decisions**

674 In the present study, previously reported heart slowing with conscious perception
675 (Park et al., 2014; Cobos et al., 2019; Motyka et al., 2019) was replicated and in
676 addition to it observed to be enhanced for unconfident decisions. Greater heart
677 slowing for unconfident decisions suggests the involvement of another mechanism
678 determining heart rate deceleration compared to the unimodal distribution of hits in
679 diastole which was absent for unconfident hits. Increased heart slowing for
680 unconfident decisions might be associated with uncertainty, because heart slowing
681 has been reported for the violation of performance-based expectations in a learning
682 paradigm (Crone et al., 2003), for errors in a visual discrimination task (Łukowska et
683 al., 2018), and for error keystrokes by pianists (Bury et al., 2019).

684

685 **Inspiration locking to stimulus onsets**

686 Localizing stimulus onsets in the respiratory cycle revealed that inspiration onsets
687 locked at the expected stimulus onset independent of stimulus presence, detection,
688 and decision confidence. Circular variance was lower for hits than misses, indicating
689 a more pronounced locking went along with a higher likelihood of hits. For the first
690 thirty trials, the difference to the mean angle of the first block showed a linear
691 decrease, suggesting that participants adapted their respiration rhythm to the
692 paradigm in the beginning. Respiratory cycles accompanying misses had a significant
693 longer duration than hits.

694 These observations support the notion that inspiration is tuning the sensory
695 system for incoming information (Perl et al., 2019). Recently, it has been shown that
696 inhale onsets were locked to different cognitive task onsets, which increased task-

specific brain activity and performance in a visuospatial perception task (Perl et al., 2019). Neural activity in piriform cortex, amygdala, and hippocampus synchronized with respiration and had its oscillatory power peak during nasal inspiration, when fearful face detection was faster, and memory encoding and retrieval was enhanced compared to expiration (Zelano et al., 2016). While we also observed locking of inhale onsets to our detection task and pronouncedly to stimulus detection, future studies could investigate whether this respiratory pattern also drives the brain activity into an optimal state for conscious tactile perception. For the visuospatial perception task by Perl et al. (2019), decreased alpha power has been observed in postcentral and parahippocampal gyrus during inspiration compared to expiration. Analogously, lower pre-stimulus alpha power in central brain areas (Mu rhythm) has been associated with higher neural excitability reflected in improved conscious tactile perception (Schubert et al., 2009; Nierhaus et al., 2015; Craddock et al., 2017; Forschack et al., 2020; Stephani et al., 2021).

Meanwhile, it is unclear whether longer respiratory cycles for misses in our study are a result of less pronounced inspiration locking or a consequence of missing the stimulus. Future studies with longer interstimulus intervals would be able to dissect whether the respiratory cycle duration is a determinant or consequence of undetected near-threshold trials. For now, we can state that participants adapted their respiratory rhythm to the paradigm and showed this more consistently in detected near-threshold trials.

Conclusion

We show that the two predominant body rhythms differentially modulate conscious tactile perception. Cardiac cycle effects seem to be grounded on higher cognitive processes compatible with an interoceptive predictive coding account. Phase locking of respiration seems to facilitate conscious tactile perception by tuning the inspiration phase to optimize detection task performance.

References

Al E, Iliopoulos F, Forschack N, Nierhaus T, Grund M, Motyka P, Gaebler M, Nikulin VV, Villringer A (2020) Heart-brain interactions shape somatosensory perception and evoked potentials. Proc Natl Acad Sci USA 7:201915629.

Allen M, Levy A, Parr T, Friston, K (2019) In the body's eye: the computational anatomy of interoceptive inference. bioRxiv 603928. doi: 10.1101/603928

Azzalini D, Rebollo I, Tallon-Baudry C (2019) Visceral Signals Shape Brain Dynamics and Cognition. Trends Cogn Sci 23:488–509.

Babo-Rebelo M, Richter CG, Tallon-Baudry C (2016) Neural Responses to Heartbeats in the Default Network Encode the Self in Spontaneous Thoughts. J Neurosci 36:7829–7840.

Benjamini Y, Hochberg Y (1995) Controlling the False Discovery Rate: A Practical and Powerful Approach to Multiple Testing. Royal Statistical Society, Series B Methodological 57:289–300

Brener J, Kluvitse C (1988) Heartbeat detection: judgments of the simultaneity of external stimuli and heartbeats. Psychophysiology 25:554–561.

Bury G, García-Huéscar M, Bhattacharya J, Ruiz MH (2019) Cardiac afferent activity modulates early neural signature of error detection during skilled performance. NeuroImage 199:704–717.

Cobos MI, Guerra PM, Vila J, Chica AB (2019) Heart-rate modulations reveal attention and consciousness interactions. Psychophysiology 56:e13295.

Craddock M, Poliakoff E, El-deredy W, Klepousniotou E, Lloyd DM (2017) Pre-stimulus alpha oscillations over somatosensory cortex predict tactile misperceptions. Neuropsychologia 96:9–18.

748 Critchley HD, Garfinkel SN (2015) Interactions between visceral afferent signaling
749 and stimulus processing. Front Neurosci 9:305–309.
750 Critchley HD, Harrison NA (2013) Visceral influences on brain and behavior. Neuron
751 77:624–638.
752 Crone EA, van der Veen FM, van der Molen MW, Somsen RJM, van Beek B,
753 Jennings JR (2003) Cardiac concomitants of feedback processing. Biological
754 Psychology 64:143–156.
755 Dick TE, Hsieh Y-H, Dhingra RR, Baekey DM, Galán RF, Wehrwein E, Morris KF
756 (2014) Cardiorespiratory coupling: common rhythms in cardiac, sympathetic,
757 and respiratory activities. Prog Brain Res 209:191–205.
758 Forschack N, Nierhaus T, Müller MM, Villringer A (2020) Dissociable neural
759 correlates of stimulation intensity and detection in somatosensation.
760 NeuroImage:116908.
761 Galvez-Pol A, McConnell R, Kilner JM (2020) Active sampling in visual search is
762 coupled to the cardiac cycle. Cognition 196:104149.
763 Hassanpour MS, Yan L, Wang DJJ, Lapidus RC, Arevian AC, Simmons WK,
764 Feusner JD, Khalsa SS (2016) How the heart speaks to the brain: neural activity
765 during cardiorespiratory interoceptive stimulation. Phil Trans R Soc Lond B 371.
766 Huijbers W, Pennartz CMA, Beldzik E, Domagalik A, Vinck M, Hofman WF, Cabeza
767 R, Daselaar SM (2014) Respiration phase-locks to fast stimulus presentations:
768 implications for the interpretation of posterior midline "deactivations". Hum
769 Brain Mapp 35:4932–4943.
770 Khalsa SS, Rudrauf D, Feinstein JS, Tranel D (2009) The pathways of interoceptive
771 awareness. Nat Neurosci 12:1494–1496.

772 Kingdom FAA, Prins N (2009) Psychophysics. London: Academic Press Inc.

773 Kleiner M, Brainard D, Pelli D, Ingling A, Murray R, Broussard C (2007) What's new
774 in psychtoolbox-3. Perception 36:1–16.

775 Kralemann B, Frühwirth M, Pikovsky A, Rosenblum M, Kenner T, Schaefer J, Moser
776 M (2013) In vivo cardiac phase response curve elucidates human respiratory
777 heart rate variability. Nat Commun 4:2418–2419.

778 Kunzendorf S, Klotzsche F, Akbal M, Villringer A, Ohl S, Gaebler M (2019) Active
779 information sampling varies across the cardiac cycle. Psychophysiology
780 56:e13322.

781 Lachaux JP, Rodriguez E, Martinerie J, Varela FJ (1999) Measuring phase
782 synchrony in brain signals. Hum Brain Mapp 8:194–208.

783 Macefield VG (2003) Cardiovascular and respiratory modulation of tactile afferents
784 in the human finger pad. Exp Physiol 88:617–625.

785 Motyka P, Grund M, Forschack N, Al E, Villringer A, Gaebler M (2019) Interactions
786 between cardiac activity and conscious somatosensory perception.
787 Psychophysiology 56:469–13.

788 Nierhaus T, Forschack N, Piper SK, Holtze S, Krause T, Taskin B, Long X, Stelzer J,
789 Margulies DS, Steinbrink J, Villringer A (2015) Imperceptible somatosensory
790 stimulation alters sensorimotor background rhythm and connectivity. J Neurosci
791 35:5917–5925.

792 Ohl S, Wohltat C, Kliegl R, Pollatos O, Engbert R (2016) Microsaccades Are
793 Coupled to Heartbeat. J Neurosci 36:1237–1241.

794 Oldfield RC (1971) The assessment and analysis of handedness: the Edinburgh
795 inventory. Neuropsychologia 9:97–113.

796 Park H-D, Barnoud C, Trang H, Kannape OA, Schaller K, Blanke O (2020) Breathing
797 is coupled with voluntary action and the cortical readiness potential. Nat
798 Commun 11:289–8.
799 Park H-D, Correia S, Ducorps A, Tallon-Baudry C (2014) Spontaneous fluctuations
800 in neural responses to heartbeats predict visual detection. Nat Neurosci 17:612–
801 618.
802 Perl O, Ravia A, Rubinson M, Eisen A, Soroka T, Mor N, Secundo L, Sobel N (2019)
803 Human non-olfactory cognition phase-locked with inhalation. Nat Hum Behav
804 3:501–512.
805 Power JD, Lynch CJ, Dubin MJ, Silver BM, Martin A, Jones RM (2020)
806 Characteristics of respiratory measures in young adults scanned at rest,
807 including systematic changes and “missed” deep breaths. NeuroImage
808 204:116234.
809 Ring C, Brener J (1992) The temporal locations of heartbeat sensations.
810 Psychophysiology 29:535–545.
811 Savitzky A, Golay MJE (1964) Smoothing and differentiation of data by simplified
812 least squares procedures. Analytical Chemistry 36:1627–1639.
813 Schubert R, Haufe S, Blankenburg F, Villringer A, Curio G (2009) Now you'll feel it,
814 now you won't: EEG rhythms predict the effectiveness of perceptual masking. J
815 Cognitive Neurosci 21:2407–2419.
816 Seth AK, Friston KJ (2016) Active interoceptive inference and the emotional brain.
817 Phil Trans R Soc Lond B 371.

818 Stephani T, Hodapp A, Jamshidi Idaji M, Villringer A, Nikulin VV (2021) Neural
819 excitability and sensory input determine intensity perception with opposing
820 directions in initial cortical responses. bioRxiv 2020.11.27.401430.
821 doi:10.1101/2020.11.27.401430
822 Tass P, Rosenblum MG, Weule J, Kurths J, Pikovsky A, J V, Schnitzler A, Freund H-
823 J (1998) Detection of n:m Phase Locking from Noisy Data: Application to
824 Magnetoencephalography. Phys Rev Lett 81:3291–3294.
825 Yates AJ, Jones KE, Marie GV, Hogben JH (1985) Detection of the heartbeat and
826 events in the cardiac cycle. Psychophysiology 22:561–567.
827 Zelano C, Jiang H, Zhou G, Arora N, Schuele S, Rosenow J, Gottfried JA (2016)
828 Nasal Respiration Entrains Human Limbic Oscillations and Modulates Cognitive
829 Function. J Neurosci 36:12448–12467.
830 Łukowska M, Sznajder M, Wierzchoń M (2018) Error-related cardiac response as
831 information for visibility judgements. Scientific Reports 8:1131.